



SYNTHESIS AND APPLICATION OF COPPER FERRITE NANOPARTICLES IN PHOTO-CATALYTIC DEGRADATION OF ORGANIC DYES: A STEP TOWARDS SUSTAINABLE ENVIRONMENT

Santosh Jengathe^{*1}, Nilesh Gandhare², Parvez Ali³, Mangesh B. Thakre⁴,
Kailas A. More², Nilesh G. Jadhao²

¹Department of Chemistry, Tai Golwalkar Mahavidyalaya, RTM Nagpur University, Ramtek, India

²Department of Chemistry, Nabira Mahavidyalaya, RTM Nagpur University, Katol, India

³Center for Health Studies, Prince Sultan Military Medical City, Riyadh, Saudi Arabia

⁴D. R. B. Sindhu Mahavidyalaya, Nagpur, India

*Corresponding author: spjengathe@gmail.com, nilkanth81@gmail.com

ABSTRACT

Water pollution caused due to organic dyes from various industries is a serious concern to the environment nowadays. Along with their severe toxicity to aquatic animals and humans, azo dyes are responsible for making up more than half of the dyes pollution. In this study, we have reported a cost effective, energy efficient, and environmentally benign method to degrade Methyl Orange and Rhodamine B dyes, using Copper Ferrite (CuFe₂O₄) nanoparticles as a photo catalyst. We have synthesized magnetic spinel copper ferrite (CuFe₂O₄) nanoparticles by co-precipitation method. The synthesized copper ferrite nanoparticles were characterized using FT-IR, XRD, SEM and TGA analysis. The synthesized nanoparticles consisted of equimolar mixture of CuO and α -Fe₂O₃ revealed from XRD studies. The diffraction pattern exhibited the corresponding Braggs reflections of these two oxides (Tetrahedral- CuFe₂O₄ and Cubic-CuFe₂O₄), with an average size of 15 nm. The efficacy of synthesized nanoparticles as photo catalyst has been demonstrated in the degradation of Rhodamine B and Methyl Orange under UV (Tungsten lamp light) irradiation. It was found that the adsorption of dyes onto the catalyst accelerated the degradation process. The percent degradation for Rhodamine B and Methyl Orange was found to be 92.88% and 86.04 % respectively in UV irradiation.

Keywords: CuFe₂O₄ NPs, Methyl Orange, Rhodamine B, Photo catalysis, Degradation.

1. INTRODUCTION

Increasing urbanization is a sign of growth, but the maintaining the balance of nature with it, is a sign of advancement and longevity of growth. However, as correctly said by Theodore Levitt, "Anything in excess is poison" is true in this case. As industries are increasing, the waste generated is also increasing. The environmental pollution has become a prominent issue with a detrimental influence on human life. The discharge of effluents from the various industries such as plastic, rubber, textile, dye manufacturing, leather, cosmetics and so on release non-biodegradable, toxic, and carcinogenic chemicals and dyes in the nearest water bodies and environment, which affects both living organisms of aquatic ecosystems and human health [1-2]. The disastrous conditions about industrial pollutants are that they consist of various dyes with high chemical stability and become challenging to decompose. It leads to generation of hazardous by-products through the

chemical processes like oxidation, hydrolysis, or other reactions [3]. Organic dyes, especially Rhodamine B and Methyl orange, are mainly used in the textile, paper, synthetic leather and food industry due to high chemical stability [4]. Rhodamine B is also a familiar water tracer fluorescent [5], which is harmful to living systems. Its exposure causes acute symptoms such as burning of the eyes, excessive tearing, nasal burning and itching, chest pain/tightness and burning, rhinorrhoea, cough, burning of the throat, headache, and nausea [6]. Its carcinogenic toxicity and reproductive effects to humans and animals have been proved experimentally [7]. Methyl Orange (MO) is a mono-azo dye widely used for estimating the alkalinity of water and as an indicator for titrating strong acids and bases. Due to the ionic nature of MO, the dye is non-volatile and less susceptible to aerobic biodegradation in soil and water. In addition, it may be adsorbed to sediments and clay and mineral surfaces in water [8]. Once in the body, MO can

undergo reductive azo-bond cleavage through reductive enzymes present in the liver and form toxic aromatic amines that can cause intestinal cancer [9]. Thus, sound scientific technical approaches are needed to reduce and eliminate the harmful effects of these pollutants on the environment and follow stringent environmental regulations. Consequently, the development of efficient processes for removal of dyes from wastewater has gained a great deal of attention. Numerous, physical [10], chemical [11] and biological [12] traditional treatment methods for removing azo dyes in wastewater methods have been explored in the past decades. Although these methods are effective in removing organics contaminants, complete decomposition is not reached. In most of the cases, there was absorption of dyes on absorbent only. Furthermore, due to high production cost and generation of extra impurities, limit their practical applications. Thus, it is necessary to develop alternative environmental-friendly approaches that are expeditious, inexpensive and efficient. In the recent years, advanced oxidation process (AOP) by photo catalysis has been emerged as one of the most promising processes in degrading complex organic compounds in polluted water [13]. Photo catalysis can be conveniently applied for degradation of dye pollutants without secondary pollution owing to the complete mineralization of organic dyes into mineral acids, H₂O, and CO₂ [14]. Metal semiconductor materials, such as TiO₂ [15], ZnO [16], Fe₂O₃ [17] and Cu₂O [18], are used as a photo catalyst.

Thus, researchers work towards nanotechnology as a new promising manner for the degradation of dyes. Nanoparticles (NPs) refer to nanoscale materials with sizes between 1nm and 100nm and show superior properties based on dimensions, distribution, morphology, and large surface-to-volume ratio [19]. These unique functional properties make nanomaterials a capable candidate for various applications in medicine, food, and engineering [20]. In recent years, metal and metal oxide nanoparticles were very encouraging materials applied in several fields due to their numerous valuable properties, such as catalytic, optical, magnetic, and electrical properties. Metal and metal oxide nanoparticles were used in various fields such as light emitting devices, biomedicine, soil stabilization, catalysis, water treatment, transparent, conductive contacts, piezoelectric transducers, laser deflectors, solar cells, biosensors, and gas sensors [21]. Metal oxides can adopt a vast number of structural geometries

with an electronic structure that can exhibit metallic, semiconductor or insulator character and there for play a very important role in many areas of chemistry, physics and material science [22]. Compared to other potential photo catalysts, iron oxides are plentiful in nature and environmentally benign. Spinel ferrites, with a general formula of MFe₂O₄, where M represents a metal Cation, are chemically and thermally stable magnetic materials that have been used for many applications. Their magnetic properties make them useful in magnetic resonance imaging (MRI), electronic devices, information storage, and drug delivery. Other applications of ferrites include adsorbents for the removal of toxic substances, including gases, the treatment of heavy metal containing waste, chemical sensors, and pigments [23-24].

Ferrites possess important photo catalytic properties for many industrial processes, including oxidative dehydrogenation of hydrocarbons, decomposition of alcohols and hydrogen peroxide, treatment of exhaust gases, oxidation of compounds such as CO, H₂, CH₄ and chlorobenzene, hydroxylation of phenol, alkylation reactions, hydride sulphurization of crude petroleum, and the catalytic combustion of methane. The presence of different metals in the lattice structure can modify the redox properties of the ferrites from various composite photo catalysts. Another advantage of using ferrites is their magnetic properties. Iron (III) oxides are highly magnetic materials, and therefore so are ferrites [25]. When ferrites are used alone as photo catalysts or in combination with others, they can therefore be easily separated from the reaction mixture. Ferrites of the form MFe₂O₄ commonly include metal cations such as Ba²⁺, Ca²⁺, Co²⁺, Cu²⁺, Mg²⁺, Mn²⁺, Fe²⁺, Sr²⁺, Ni²⁺, and Zn²⁺. Ferrites alone have been shown to be effective photo catalyst by utilizing light energy to create e⁻/h⁺ pairs on the photocatalytic surface [26].

There are several works dealing with the use of spinel ferrite catalysts (MFe₂O₄) for the photocatalytic degradation of Rhodamine B (RhB, Fig. 1) and Methyl Orange (MO, Fig. 2) dyes in the water treatment. Those are MnFe₂O₄, CoFe₂O₄, FeFe₂O₄ [27], CaFe₂O₄ [28], ZnFe₂O₄ [29], ZnO/ZnFe₂O₄ [30] etc; with percent degradation ranges from 75 to 100%. However, many of them, suffered from one or more drawbacks like multistep tedious synthetic processes, incomplete degradations, pH issues, high production cost of catalysts, requirement of metal oxides, montmorillonite and active carbon in combination support, heat treatments above 800°C etc.

Thus, to minimise the mentioned drawbacks and associated health hazards on the ecosystems, in this work, we have reported the degradation of an aqueous solution of the organic dyes, Rhodamine B (RhB, Fig. 1) and Methyl Orange (MO, Fig. 2) in the presence of H_2O_2 by heterogeneous photo catalysis using synthesized Magnetic spinel copper ferrites ($CuFe_2O_4$). The effect of different operating parameters such as the amount of

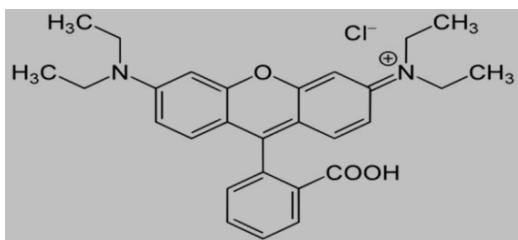


Fig. 1: Rhodamine B (RhB)

photo catalyst, H_2O_2 concentration, light intensity, radiation source, and reutilization of the photo catalyst on successive dye discoloration experiments was also investigated. The catalytic activity in the presence of UV of Copper Ferrite nanoparticles is studied at different time intervals, the rate constant and extent of decolourization and degradation was modelled using existing equations.

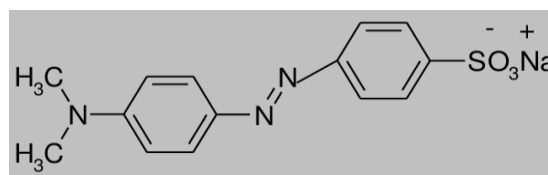


Fig. 2: Methyl Orange (MO)

2. MATERIAL AND METHODS

2.1. Materials

Copper Nitrate Pentahydrate (98%), Ferric Nitrate Nanohydrate (99%), Cetyl trimethyl ammonium bromide (CTAB-99%), Sodium hydroxide pellets (98%), Rhodamine B (97%), Methyl Orange dye (98%) and Hydrogen Peroxide (30%) were purchased from S. D. Fine chemicals Ltd. India and used without further purification.

2.2. Characterization Techniques

Crystallite phases of the obtained Copper Ferrite materials were identified by X-ray diffraction (XRD) measurements with (Rigaku-Miniflex 300 and XPERT-PRO) X-Ray diffractometer using Copper $K\alpha$ radiation in the 2θ range of 1 to 100° . A scanning electron microscope (Carl Zeiss EVO 18, Germany) has been used to investigate the particle size and morphology of the samples. Wavelength absorption was conducted by UV-Vis (Shimadzu Spectrophotometer UV 240). Energy dispersive X-ray analyser Oxford INCA Energy 250 EDS System determined elemental composition of the catalyst. A FT-IR spectrum was recorded using Bruker Alpha E spectrometer with ZnS ATR crystal.

2.3. Procedure for the synthesis of Copper Ferrite nanoparticles

In a beaker, 10 grams Cetyltrimethylammonium bromide was dissolved in 200 ml distilled water and it was stirred on magnetic stirrer till CTAB was completely dissolved in distilled water at $60^\circ C$ and transparent solution was obtained. In separate beakers,

5 grams of Copper Nitrate and 5 grams of Ferric Nitrate each was dissolved in 80ml distilled water. Both the solutions were added simultaneously to the previously prepared transparent solution of CTAB. The mixture was kept stirring for 15 minutes. An orange coloured solution was appeared. In the next step, 20% NaOH solution (20g in 100ml distilled water) was added drop wise manner and stirring was continued for 30 minutes at $90^\circ C$. A dark brown precipitate was obtained; after settling the reaction mixture for 10 minutes. The obtained precipitate was filtered, washed with double distilled water, ethanol and again washed with double distilled water till neutral pH was obtained. The washed precipitate was kept for drying in hot air oven at $80^\circ C$ for 12 hours. After drying, the precipitate was crushed into fine powder using clean mortar and pestle. The fine powder was kept in muffle furnace for 5 hours at $700^\circ C$ for calcination. Finally, dark brown coloured powder of Nano particles was obtained. Fig. 3 shows a graphical scheme for the preparation of $CuFe_2O_4$ NPs by co-precipitation method.

2.4. Preparation of dye solutions

Dye solutions (Rhodamine B and Methyl Orange) of 10 ppm concentration each were prepared, as a stock solution. 0.1 gram of each dye was dissolved in 1 litre of distilled water separately. 50 ml of this stock solution was taken out and 0.3g of copper ferrite nanoparticles was added to this solution. These dye solutions was covered with carbon paper and allowed to stir for 30 minutes in order to maintain adsorption-desorption equilibrium. After 30 minutes, the mixture was taken in

a reactor in order to irradiate reaction suspension in UV radiations. In this way, same type of system was prepared for methyl orange dye in order to irradiate

with UV. UV irradiation was performed under handmade wooden box fitted with cylindrical mercury lamp from 400W at 366nm.

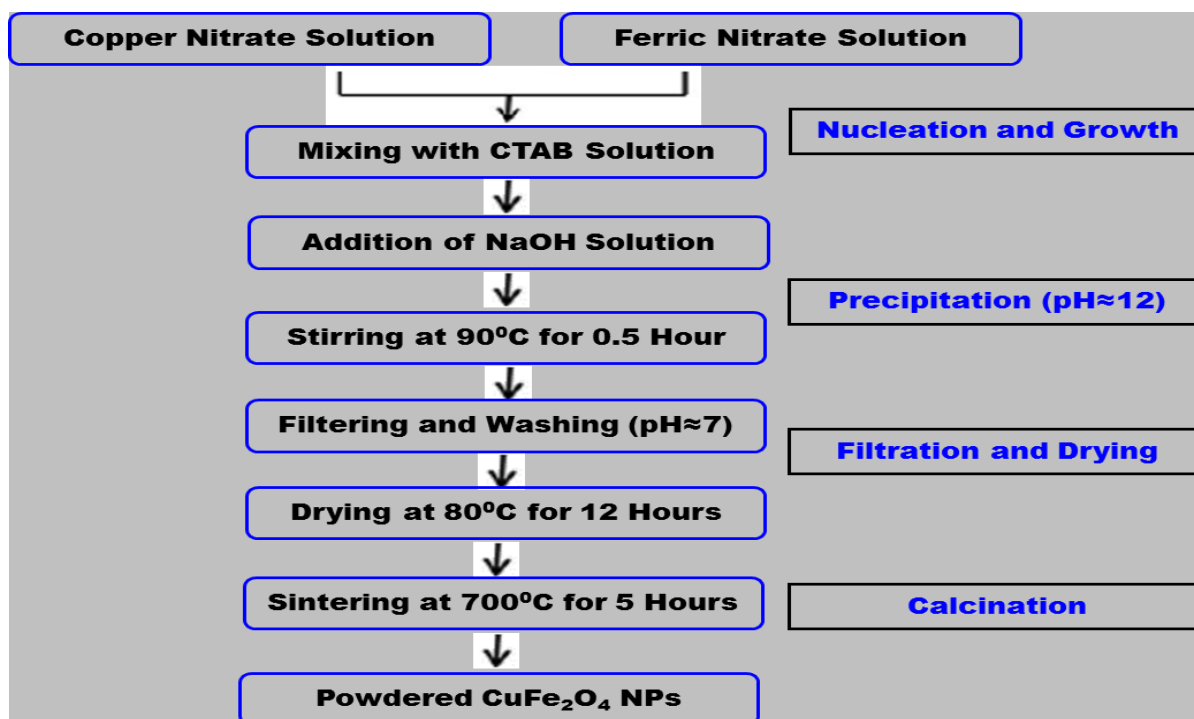


Fig. 3: Schematic diagram for the synthesis of copper ferrite nanoparticles by co-precipitation method

2.5. Photocatalytic degradation of dyes

4 ml of each dye solution were pipetted out into syringe with the help of needle and filter paper in order to separate out the catalyst particles and dye solution. The absorbance of dye solution was recorded on UV-visible spectrometer in order to evaluate the photocatalytic degradation of dyes (Rh and MO). Absorbance was noted at every 30 minutes of intervals for each irradiation, until 180 minutes duration to study percent degradations. Percentage (%) degradation of dye was calculated by the below formula;

$$\% \text{ Degradation} = (1 - A_t/A_0) \times 100$$

Where, A_t is absorbance after time t and A_0 is the absorbance before degradation.

3. RESULTS AND DISCUSSION

3.1. Characterization of Synthesized Copper Ferrite nanoparticles

The Copper Ferrite nanoparticles were synthesized by Co-precipitation Method. The synthesized copper ferrite were characterized through various spectroscopic techniques which includes Fourier transform infrared spectroscopy (FT-IR), X-ray diffraction spectroscopy

(XRD), Scanning electron microscopy (SEM) and Thermo gravimetric analysis (TGA).

3.1.1. FT-IR Studies

Fourier transform infrared spectroscopy includes the interplay of photons with the species in the given sample which shows transfer of to or from the samples through de-excitation or vibrational excitation, which is exploited for characterization. These vibrational frequencies provide the facts of chemical bonding in the sample. Fig. 4 shows FT-IR spectra of Copper Ferrite nanoparticles. FT-IR spectroscopy was carried out in order to ascertain the purity and nature of metal or metal ferrite nanoparticles. FT-IR spectrum of CuFe_2O_4 nanoparticles was recorded in the range of 400-4000 cm^{-1} . The weak absorption band observed at 1626 cm^{-1} , is due to the bending vibration of absorbed water and the absorption band at 3431 cm^{-1} is because of the O-H stretching mode. However, the main bands that characterize the formation of spinel phase are located at 875 and 643 cm^{-1} , which are associated with the vibrations of Cu-O and Fe-O bonds, respectively.

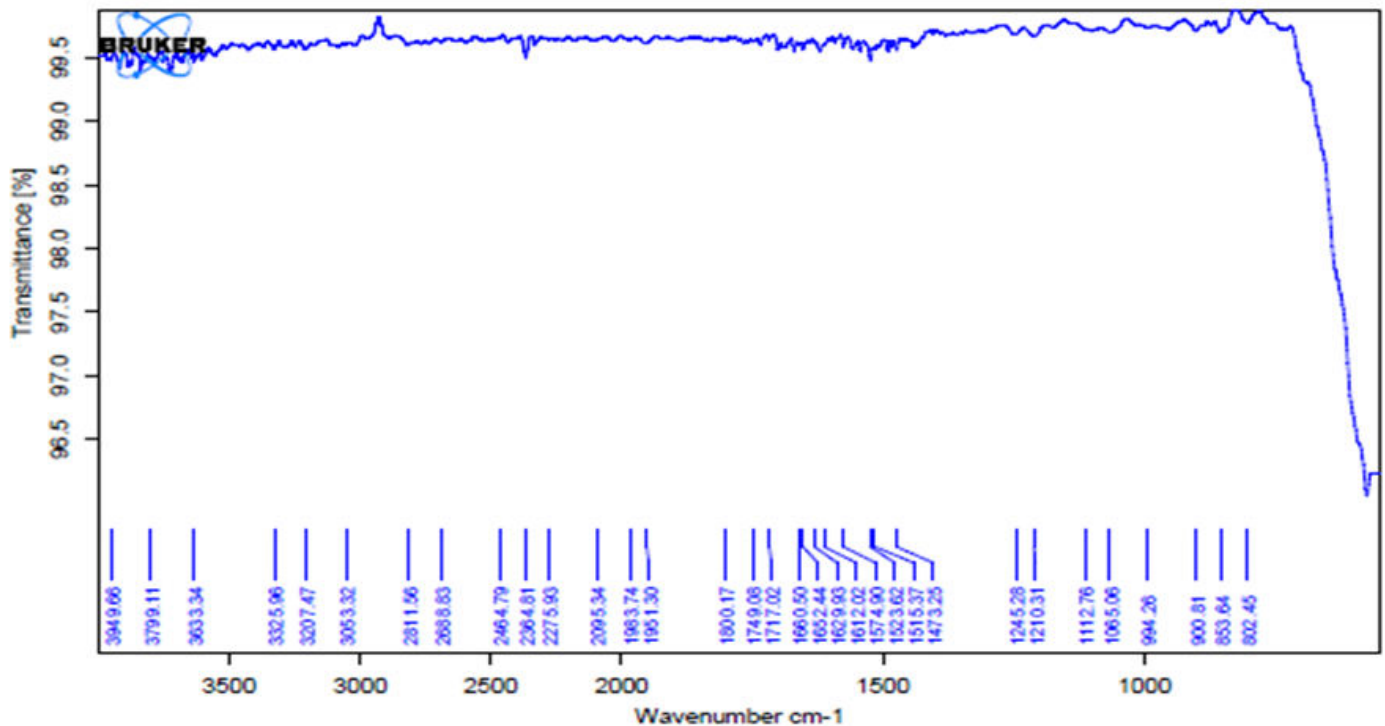


Fig. 4: FTIR spectrum of copper ferrite nanoparticles

3.1.2. X ray diffraction studies

Powder X ray diffraction studies were used to determine the crystallite size of Copper Ferrite nanoparticles, which is calculated using Scherer's equation. By comparing the position of the peaks in the diffracted beam with the standard by JCPDS file, the unknown sample can be identified.

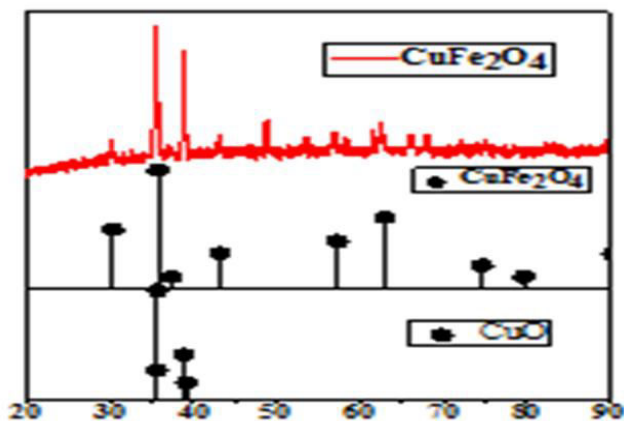


Fig. 5: XRD spectrum of copper ferrite nanoparticles

Fig. 5 shows the representative XRD patterns of synthesized CuFe_2O_4 NPs. X-ray diffraction study shows the nanoparticles consist of equimolar mixture of CuO

and $\alpha\text{-Fe}_2\text{O}_3$ (Mixed oxides) and as expected, the diffraction pattern exhibit the corresponding Bragg's reflections of these two oxides. The expected Bragg's reflections of the tetrahedral- CuFe_2O_4 and Cubic- CuFe_2O_4 are (211) and (311) respectively.

3.1.3. Scanning Electron Microscope Studies

The Scanning Electron Microscope is an instrument that produces a largely magnified image by using electrons instead of light to form an image. From SEM analysis, we can surface morphology and shape of the sample. Microscopic studies were performed to examine the surface of materials. SEM analysis illustrated information about the surface and a bulk area of synthesized CuFe_2O_4 NCs. SEM analysis (Fig. 6) provides images ranging from $1\mu\text{m}$ to $10\mu\text{m}$. As we know that it is very difficult to keep particles in non-agglomerated form, synthesized CuFe_2O_4 NCs shows irregular agglomeration of small particles into a tight mass, which was clearly seen in these images (Fig. 6).

3.1.4. Thermogravimetric Analysis

The synthesized NPs was examined by thermal analysis technique to evaluate their thermal stability, when it is heated at 1000°C . Two stage of thermal decomposition were found for NCs. The weight loss at $31\text{-}150^\circ\text{C}$ due

to the evaporation of water molecules, and then it has followed by loss of organic compound started to vaporize in the form of CO_2 about 0.75. The weight was

lost about 4.76 from 150-1000°C. Thus, during heating at such high temperature 5.51 % total weight loss with formation of stable crystalline NCs was observed.

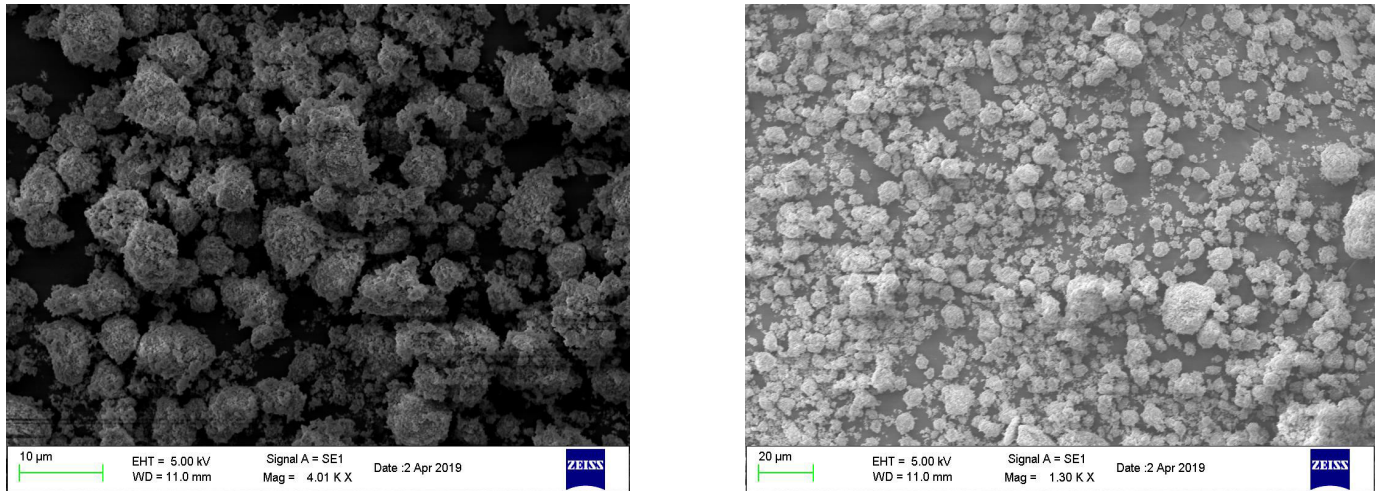


Fig. 6: SEM images of synthesized CuFe_2O_4 NPs

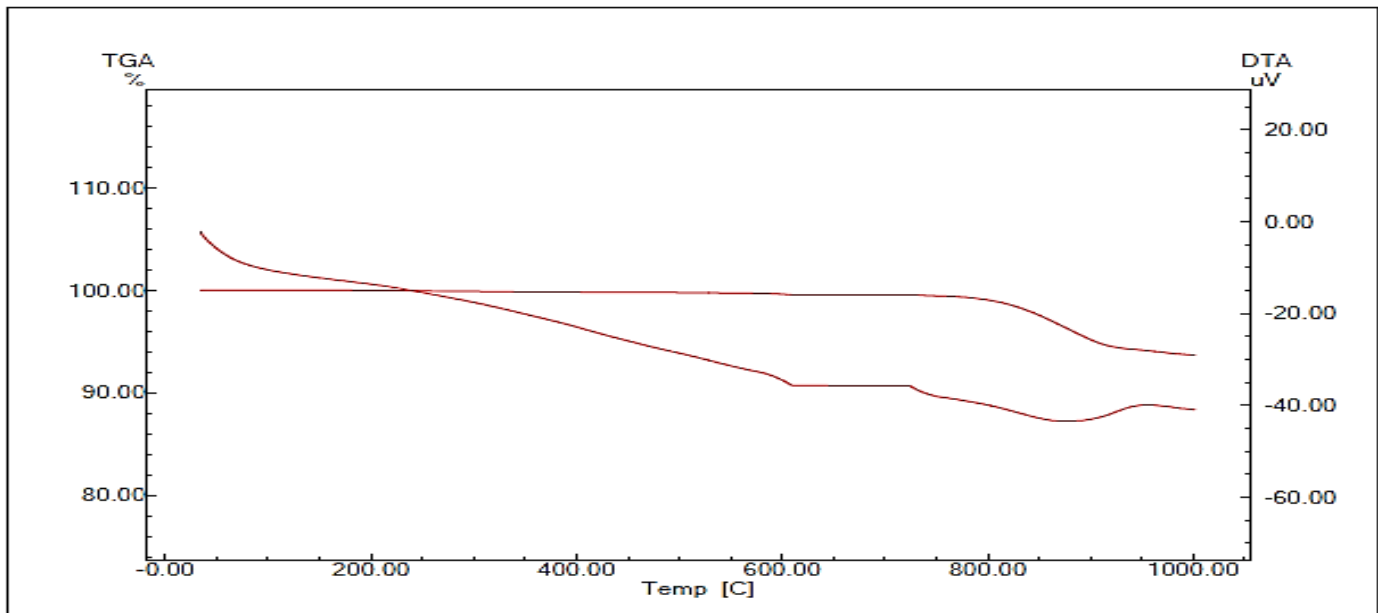


Fig. 7: TGA for the thermal decomposition of CuFe_2O_4 NPs

3.2. Photocatalytic Activity

Photo degradation experiments were carried out with irradiation of the dye solutions under UV light (Tungsten lamp light source). The extent of dyes degradation was monitored using UV-Vis Spectroscopic technique. The Photocatalytic degradation catalysed by micro spindle Y- CuFe_2O_4 NPs was investigated by degradation of the dye pollutants Rh and MO. The relative absorption maximum for RhB and MO was

observed at 555 and 430 nm using a UV- Visible Spectrophotometer. It was observed that in the absence of photo catalyst, degradation process takes very long time of about 4-5hr. The absorbance of dye solutions at an initial (A_0) and after a specific time (A_t) was used in Beer's law to calculate degradation percentage:

$$\% \text{ Degradation} = (1 - A_t/A_0) \times 100$$

The apparent rate constant of the degradation reaction catalysed by 3 mg/100 ml of Y- CuFe_2O_4 NPs was

calculated using tungsten light lamp irradiation by $\ln(A_t/A_0) = k t$, where k is apparent rate constant (min^{-1}). After the addition of γ - CuFe_2O_4 NPs photo catalyst to the dye solutions, adsorption-desorption equilibrium was reached, leading to the enhancement of Photo degradation of dyes. The degradation efficiencies of RhB and MO dyes for 180 minutes in UV (Tungsten lamp light irradiation) are tabulated in table 1 and 2.

Therefore, an enhancement in the degradation efficiency of dyes has been achieved by the addition of micro spindle γ - CuFe_2O_4 NPs. The increase in decolourization rate was observed due to an increase in the availability of active sites and thus an increase in the density of particles in the illumination area. The detailed photocatalytic degradation efficiency of dyes in the Tungsten lamp light irradiation in presence of micro spindle γ - CuFe_2O_4 NPs is shown in Fig.s 8-10, which indicates the increased photocatalytic degradation efficiency, because of the influence of many factors and their mutual effects due to heterogeneous photo catalysis reactions. We found that degradation of dyes follows a pseudo first order kinetic expression due to the straight line obtained by plotting ratio of log of absorbance at time t and initial absorbance (A_t/A_0) against irradiation time (Fig. 11). Many reports indicated that the kinetic model for heterogeneous photo catalysis follow the Langmuir-Hinshelwood expression. It was observed that after irradiation for 3 hours, about 88.92% of RhB and 86.02% of MO was degraded in the presence of CuFe_2O_4 NPs photo catalyst. The observed photocatalytic degradation order

in the presence of micro spindle γ - CuFe_2O_4 NPs with UV (Tungsten lamp light) irradiation follows ($\text{RhB} > \text{MO}$). This was attributed to light irradiation on the degradation efficiency on organic dyes.

Table 1: Degradation efficiencies of Rhodamine B as a dye over micro spindle γ - CuFe_2O_4 NPs in different time interval under UV (tungsten lamp light source) light irradiation

Time (Minutes)	% Degradation
0 min	0 %
30 min	13.71 %
60 min	22.33 %
90 min	40.91 %
120 min	49.73 %
150 min	75.31 %
180 min	92.88 %

Table 2: Degradation efficiencies of Methyl Orange as a dye over micro spindle γ - CuFe_2O_4 NPs in different time interval under UV (tungsten lamp light source) light irradiation

Time (Minutes)	% Degradation
0 min	0 %
30 min	13.01 %
60 min	26.42 %
90 min	35.31 %
120 min	56.27 %
150 min	72.70 %
180 min	86.04 %

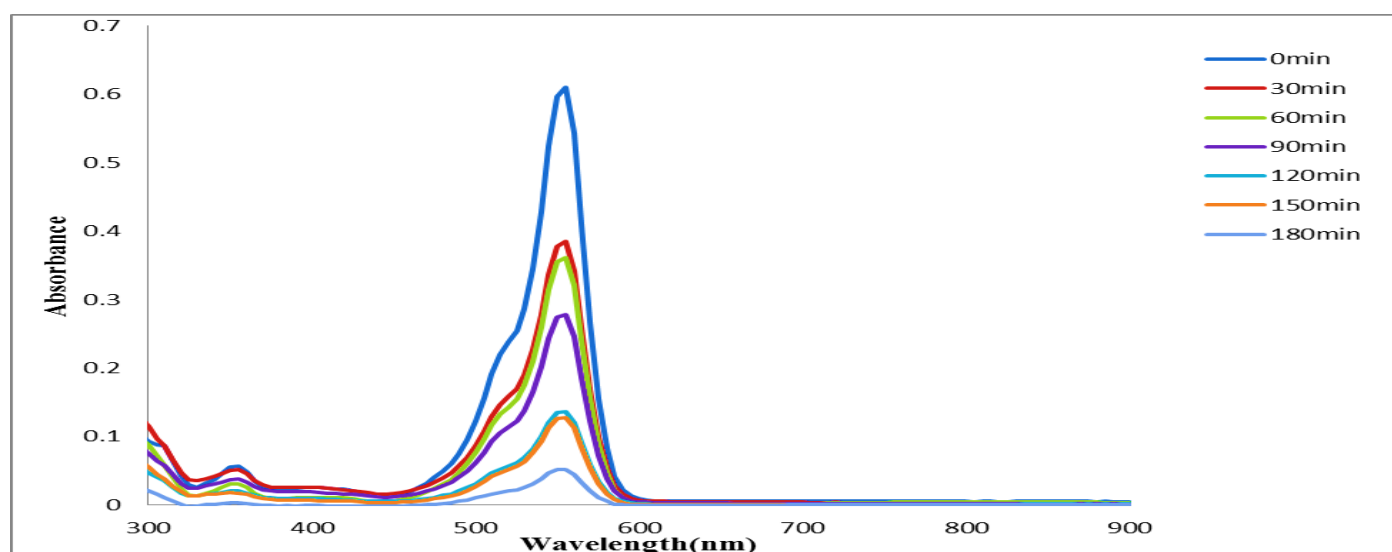


Fig. 8: Plot of Absorbance v/s Wavelength of RhB under Tungsten lamp light source irradiation

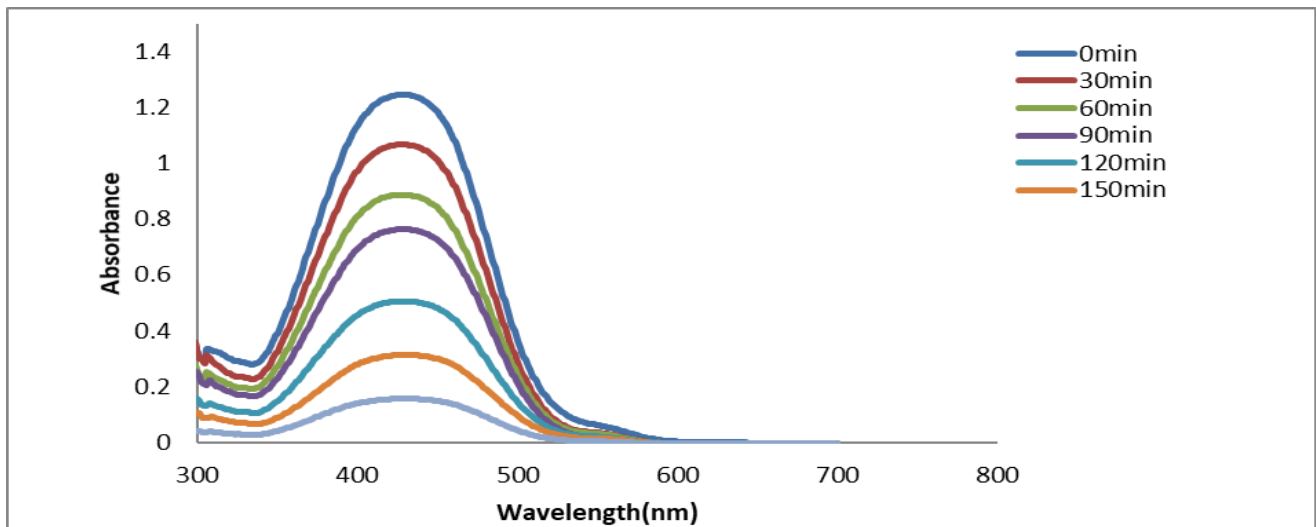


Fig. 9: Plot of Absorbance v/s Wavelength of MO under Tungsten lamp light source irradiation

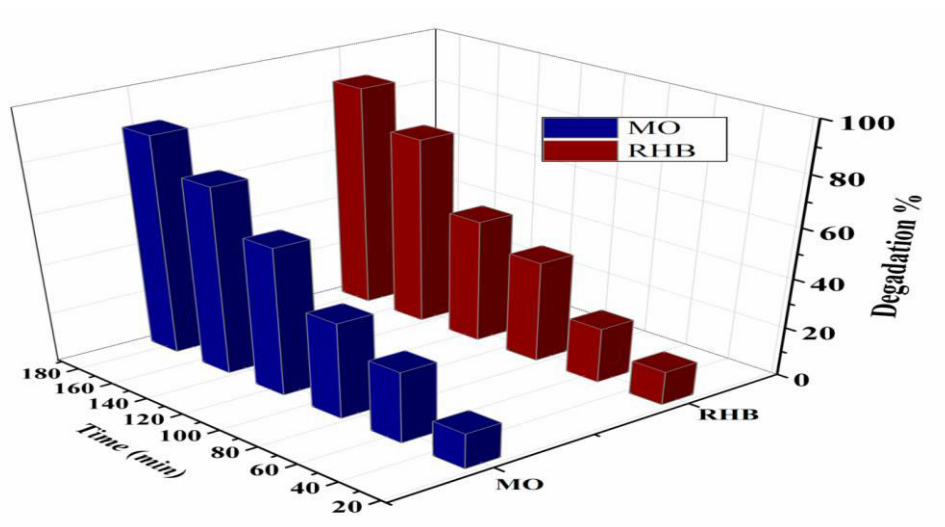


Fig. 10: Plot of % Degradation v/s Time of RhB and MO under irradiation

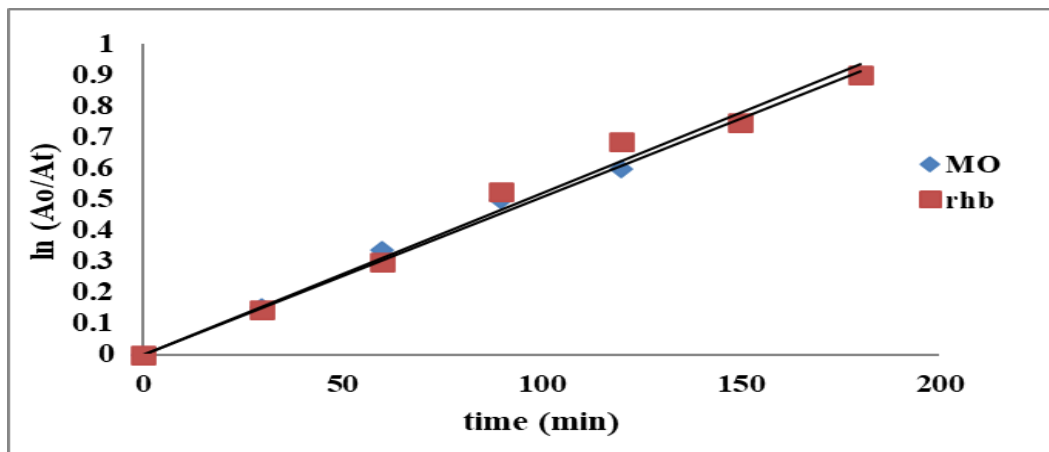
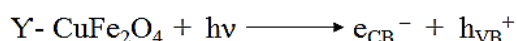


Fig. 11: Plot of ln (A₀/A_t) v/s Time (minutes) of RhB and MO

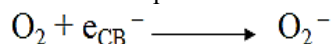
3.3. Plausible Mechanism for CuFe₂O₄ NPs assisted Photodegradation of RhB and MO

A tentative mechanistic rationale for CuFe₂O₄ NPs assisted photo degradation of RhB and MO under UV light is shown in reactions (1-5), based on the literature [31]. In the UV light irradiation, excitation of the electron from the valence band (VB) to conduction band (CB) of CuFe₂O₄ NPs occurs leading to the generation of the electron and hole in the VB and CB, respectively (reaction 1). The electrons transferred in the CB react with O₂ molecules to form oxidative species super oxide radical (O₂⁻) (reaction 2). Furthermore, photo induced holes left in VB accept electrons from the hydroxyl group forming highly oxidative ·OH radicals (reaction 4), which are responsible for degradation of dyes.

- 1. Absorption of efficient photons by copper ferrite ($h\nu \geq E_{bg}$)



- 2. Formation of the super oxide radical anion



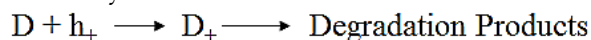
- 3. Neutralization of OH- group into OH by the hole ($H_2O \longleftrightarrow H^+ + OH^-$)_{ads} + h_{VB}^+ \longrightarrow OH + H⁺

It has been suggested that hydroxyl radical (OH) and super oxide radical (O₂⁻) are the primary oxidizing species in the photocatalytic oxidation processes. These oxidative reactions would result in the degradation of the dye or Pollutants as shown in the following reactions 4-5.

- 4. Oxidation of the organic pollutants (D=Dyes) via successive attack by OH radicals



- 5. Or by direct reaction with holes



4. CONCLUSION

The Copper Ferrite Nanoparticles were successfully synthesized using Co-precipitation method and characterized by XR-D, FT-IR, SEM, and TGA. This new material was found to be effective catalyst for the destruction of industrial dyes Rhodamine B (RhB) and Methyl Orange (MO) under the UV (Tungsten lamp light) irradiation. It was found that the adsorption of dye onto the catalyst accelerated the degradation process and hence the above dyes were easily degraded. The observed photocatalytic degradation in presence of micro spindle Y-CuFe₂O₄ NPs with UV (Tungsten lamp light) irradiation follows (Rhodamine > Methyl orange) order. This was attributed to

the light irradiation on the degradation efficiency of organic dyes. The percent degradation for Rhodamine B and Methyl Orange (MO) was found to be 92.88% and 86.04 % in UV irradiation. In this way, the use of copper ferrites obtained by Co-precipitation method from nitrate precursors becomes a promising approach for the removal of organic pollutants by photocatalytic oxidation in the presence of H₂O₂ and may constitute an alternative for total degradation of the RhB and MO dyes. Thus, it was found that the synthesized micro spindle Y-CuFe₂O₄ NPs could act as an excellent and cheap photo catalyst in degrading the pollutants, such as dyes from various industries.

5. ACKNOWLEDGEMENT

Authors would like to thank Principal, Tai Golwalkar Mahavidyalaya Ramtek, PGTD Department of Chemistry RTM Nagpur University, India, for providing the facilities for carrying out research work. Authors thank, Head, Department of Chemistry, RTM Nagpur University, Nagpur and NEERI Nagpur, VNIT Nagpur, India for FT-IR, SEM, TGA and XRD analysis respectively.

Funding

The authors of this research did not receive any funding concerning this research.

Declaration of interest

The authors report and declare that there are no financial, personal and professional conflicts of interest. The authors alone are responsible for the content and writing of the research paper.

6. REFERENCES

1. Yi S, Zou Y, Sun S, Dai F, Si Y, Sun G. *ACS Sustainable Chemistry & Engineering*, 2018; **7**:986-993.
2. Sarkar S, Banerjee A, Halder U, Biswas R, Bandopadhyay R. *Water Conservation Science and Engineering*, 2017; **2**:121-131.
3. Ameta S, Ameta R. 1st ed. *Academic Press: London*, 2018; 1-12.
4. Liu J, Peng G, Jing X, Yi Z. *Water Science and Technology*, 2018; **78**:936-946.
5. Richardson S, Willson C, Rusch K. *Ground Water*, 2004; **42**:678-688.
6. Dire D, Wilkinson J. *Journal of Toxicology: Clinical Toxicology* 1987; **25**:603-607.
7. Kornbrust D, Barfknecht T. 1985; **7**:101-120.

8. Evans L. *Environmental Science & Technology*, 1989; **23**:1046-1056.
9. Mittal A, Malviya A, Kaur D, Mittal J, Kurup L. *Journal of Hazardous Materials*, 2007; **148**:229-240.
10. Neethu N, Choudhury T. *Recent Patents on Nanotechnology*, 2018; **12**:200-207.
11. Abass A, Raof S. *Journal of Physics: Conference Series*, 2020; **1664**:012066.
12. Al-Baldawi I, Abdullah S, Almansoori A, Ismail N, Hasan H, Anuar N. *Scientific Reports*. 2020; doi: 10.1038/s41598-020-70740-5
13. Abass A, Raof S. *Journal of Physics: Conference Series*, 2020; **1664**:012066.
14. Singh J, Soni R. *Applied Surface Science*, 2020; **521**:146420.
15. Guo Q, Zhou C, Ma Z, Yang X, *Advanced Materials*, 2019; **31**:1901997.
16. Boughelout A, Macaluso R, Kechouane M, Trari M. *Reaction Kinetics, Mechanisms and Catalysis*, 2020; **129**:1115-1130.
17. Imran M, Abutaleb A, Ashraf Ali M. *Materials Letters*, 2020; **258**:126748.
18. Peerakiathajohn P, Yun J, Butburee T, Chen H, Thaweesak S, Lyu M. *Journal of Hazardous Materials*, 2021; **402**:123533.
19. Afsharian Z, Khosravi-Daran K, *Bio interface Research in Applied Chemistry*, 2019; **10**:4790-4802.
20. Afsharian Z, Khosravi-Daran K. *Biointerface Research in Applied Chemistry*, 2019; **10**:4790-4802.
21. Fernandes C, Benfeito S, Fonseca A. *Food Preservation, Academic Press: Cambridge, MA, USA*, 2017; 527-565.
22. Mallahi M, Mazinani V, Vaezi M, Shokuhfar A. *International Journal of Engineering Research*, 2014; **3**:267-270.
23. Kundu S, Gupta A. *Separation and Purification Technology*, 2006; **51**:165-172.
24. Machala L, Tucek J, Zboril R. *ChemInform* **42**:2011; doi: 10.1002/chin.201139208
25. Zhao L, Li X, Zhao Q, Qu Z, Yuan D, Liu S, Hu X, Chen G. *Journal of Hazardous Materials*, 2010; **184**:704-709.
26. Amat A, Arques A, Miranda M, Seguí S, Vercher R. *Desalination*, 2007; **212**:114-122.
27. Pereira C, Pereira A, Fernandes C, Rocha M, Mendes R, Fernández-García M, Guedes A. *Chemistry of Materials*, 2012; **24**:1496-1504.
28. EL-Rafei A, El-Kalliny A, Gad-Allah T. *Journal of Magnetism and Magnetic Materials*, 2017; **428**:92-98.
29. Patil S, Bhojya Naik H, Nagaraju G, Viswanath R, Rashmi S, Vijay Kumar M. *Materials Chemistry and Physics*, 2018; **212**:351-362.
30. Xu Y, Rao H, Wang X, Chen H, Kuang D, Su C. *Journal of Materials Chemistry A*, 2016; **4**:5124-5129.
31. Tian S, Zhang J, Chen J, Kong L, Lu J, Ding F, Xiong Y. *Industrial & Engineering Chemistry Research*, 2013; **52**:13333-13341.